PHYSICAL REVIEW A VOLUME 18, NUMBER 2 AUGUST 1978

Electron-impact excitation of metastable argon and krypton

H. A. Hyman
Avco Everett Research Laboratory, Inc., 2385 Revere Beach Parkway, Everett, Massachusetts 02149
(Received 7 April 1978)

Born cross sections have been calculated for electron-impact excitation of metastable levels of argon and krypton to higher-lying excited states. It is shown that the intermediate-coupling representation must be used to obtain reliable results. An approximate treatment of strong-coupling effects is included for the dominant *ns-np* transitions, and the applicable range and validity of the Born calculations are considered.

I. INTRODUCTION

There has been considerable recent interest in rare-gas monohalide lasers, due to their potential for high-power, high-efficiency performance. This had led to an increased understanding of the physics of rare-gas–halogen discharges. In particular, a detailed study[1] of the KrF laser discharge has shown that electron-impact excitation of the rare-gas metastables strongly affects the electron energy distribution function and the efficiency of producing the KrF* upper laser state. The relevant processes are

$$e + \mathrm{Ar}^*(3p^5 4s) \rightarrow e + \mathrm{Ar}^*(3p^5 nl)\,,$$

$$e + \mathrm{Kr}^*(4p^5 5s) \rightarrow e + \mathrm{Kr}^*(4p^5 nl)\,,$$

where nl represents higher-lying states. The $p^5 s$ state is split into four levels: $J = 0, 2$ which are truly metastable, and two levels with $J = 1$, which can radiatively decay to the ground state. Under typical laser operating conditions,[1] however, the $J = 1$ states are radiatively trapped, and therefore long lived. Consequently, all four levels are effectively metastable for the conditions of interest. Calculations have been carried out for the above processes in order to establish the magnitude of the cross sections over a broad energy range, and for comparison with and interpretation of experexperimental cross-section measurements.[2]

II. THEORY

A. Basic formulas

The first Born approximation[3] has been used for the present calculations [although an approximate treatment of strong-coupling effects has been included for the dominant s-p transitions (see Sec. III)]. The Born cross section, in units of πa_0^2, for a transition from initial state i to final state f is given by

$$Q_{if} = \frac{8}{k_i^2\,\Delta E} \int_{K_{\min}}^{K_{\max}} f_{if}(K)\, d(\ln K)\,, \tag{1}$$

where k_i^2 is the incident electron energy, $\Delta E = E_f - E_i$ is the transition energy, and $K = |\vec{k}_i - \vec{k}_f|$ is the magnitude of the momentum change of the incident electron. The quantity $f_{if}(K)$ is the generalized oscillator strength[3] (GOS), and is given by

$$f_{if}(K) = \frac{\Delta E}{K^2} \left| \left\langle \Psi_f \right| \sum_{j=1}^{N} \exp(i\vec{K}\cdot\vec{r}_j) \left| \Psi_i \right\rangle \right|^2, \tag{2}$$

where Ψ_i and Ψ_f are the initial and final wave functions of the N electron atom, respectively.

We start from a single-configuration intermediate-coupling (IC) wave function[4] for the rare-gas excited states. Expanding the IC state in terms of pure LS-coupled basis states, we obtain

$$|p^5 nl\ \Gamma J M\rangle = \sum_{SL} |p^5(^2P) nl\, SLJM\rangle \langle SLJ\ |\Gamma J\rangle\,. \tag{3}$$

In the absence of external fields, J (the total angular momentum) is a rigorous quantum number in any representation. The expansion coefficients $\langle SLJ\ |\Gamma J\rangle$ are elements of a unitary matrix, and in general are obtained by diagonalizing the spin-orbit Hamiltonian in the LS basis states.[4] Transformation matrices between various pure-coupling schemes are given in Ref. 5.

To evaluate the matrix element in formula (2) we use the well-known expansion of the plane wave in spherical harmonics:

$$\exp(i\vec{K}\cdot\vec{r}) = 4\pi \sum_{\lambda\mu} i^\lambda j_\lambda(Kr)\, Y^*_{\lambda\mu}(\hat{K})\, Y_{\lambda\mu}(\hat{r})\,, \tag{4}$$

with $j_\lambda(Kr)$ the spherical Bessel function. Substituting expressions (3) and (4) into (2), summing over final degenerate states and averaging over initial degenerate states, we obtain

$$f_{\Gamma_i J_i, \Gamma_f J_f}(K) = \frac{\Delta E}{K^2} \frac{4\pi}{2J_i+1} \sum_\lambda \left| \sum_{S_i L_i} \sum_{S_f L_f} \langle \Gamma_f J_f | S_f L_f J_f \rangle \langle p^5(^2P) n_f l_f S_f L_f J_f \| j_\lambda(Kr) Y_\lambda(\hat{r}) \| p^5(^2P) n_i l_i S_i L_i J_i \rangle \right.$$
$$\left. \times \langle S_i L_i J_i | \Gamma_i J_i \rangle \right|^2 . \quad (5)$$

The reduced matrix element is evaluated by two applications of Eq. (7.18) of Edmonds[6] to give

$$\langle p^5(^2P) n_f l_f S_f L_f J_f \| j_\lambda(Kr) Y_\lambda(\hat{r}) \| p^5(^2P) n_i l_i S_i L_i J_i \rangle$$
$$= (-1)^{J_f + S_i + L_i + L_f + l_i + l_f + 1} \delta_{S_i, S_f} \left(\frac{(2J_i+1)(2J_f+1)(2L_i+1)(2L_f+1)(2l_i+1)(2l_f+1)(2\lambda+1)}{4\pi} \right)^{1/2}$$
$$\times \begin{Bmatrix} L_f & J_f & S_i \\ J_i & L_i & \lambda \end{Bmatrix} \begin{Bmatrix} l_f & L_f & 1 \\ L_i & l_i & \lambda \end{Bmatrix} \begin{pmatrix} l_f & \lambda & l_i \\ 0 & 0 & 0 \end{pmatrix} R_\lambda(K) \quad (6)$$

with

$$R_\lambda(K) = \int_0^\infty P_{n_f l_f}(r) j_\lambda(Kr) P_{n_i l_i}(r)\, dr , \quad (7)$$

and where $P_{nl}(r)$ is the radial part of the wave function. We have assumed that the various levels of a given configuration can be described by a single radial wave function.

For $n_i s$-$n_f p$ transitions, only the $\lambda = 1$ term provides a nonvanishing contribution, and for this case it is straightforward to show from Eqs. (5)–(7) that

$$f^{(\lambda=1)}_{\Gamma_i J_i, \Gamma_f J_f}(K) = \frac{\Delta E}{K^2} \frac{3}{2J_i+1} \left(\frac{R_1(K)}{d} \right)^2 \times S(\Gamma_f J_f, \Gamma_i J_i) \quad (8)$$

with

$$d = \int_0^\infty P_{n_f p}(r) r P_{n_i s}(r)\, dr , \quad (9)$$

and with S the optical line strength[4] in atomic units. Equation (8) can be used to circumvent the spin-orbit diagonalization procedure for cases where either experimental data or intermediate-coupling calculations exist for the line strength.

Finally, for various applications it is useful to consider an average excitation cross section between two configurations, which we define as the sum over final $\Gamma_f J_f$ states and the average over initial $\Gamma_i J_i$ states. The average GOS is then given by

$$\bar{f}_{n_i l_i, n_f l_f}(K) = \frac{1}{12(2l_i+1)} \sum_{\Gamma_i J_i} \sum_{\Gamma_f J_f} (2J_i+1) f_{\Gamma_i J_i, \Gamma_f J_f}(K) . \quad (10)$$

Using Eq. (5), together with the unitary property of the expansion matrix and the orthonormality relations for the 6-J symbols,[5] we obtain

$$f_{n_i l_i, n_f l_f}(K) = \frac{\langle \Delta E \rangle}{K^2} (2l_f+1) \times \sum_\lambda (2\lambda+1) \begin{pmatrix} l_f & \lambda & l_i \\ 0 & 0 & 0 \end{pmatrix}^2 |R_\lambda(K)|^2 , \quad (11)$$

where $\langle \Delta E \rangle$ is the average transition energy (see Sec. II B). This is a one-electron formula, independent of coupling, as expected.

B. Radial wave function

The radial wave functions are determined from a semiempirical method,[7] in which the radial Schrödinger equation for the active electron is written in the form

$$\left[\frac{d^2}{dr} - \frac{l(l+1)}{r^2} + \frac{2}{r} \zeta\left(\frac{r}{a_{nl}}\right) + \tilde{E}_{nl} \right] P_{nl}(r) = 0 . \quad (12)$$

$\tilde{E}_{nl}$ is taken to be the statistically averaged experimental binding energy of the configuration, $\zeta(\rho)$ is the "effective charge" of the atomic core,[7] and a_{nl} is a radial scaling or distortion parameter and is the eigenvalue of Eq. (12) subject to the boundary conditions $P_{nl}(0) = P_{nl}(\infty) = 0$. The function $\zeta(\rho)$ is given by

$$\zeta(\rho) = (Z-N) + \sum_{j=1}^{N} \int_\rho^\infty \left(1 - \frac{\rho}{\rho'}\right) P_j^2(\rho')\, d\rho' , \quad (13)$$

with Z the nuclear charge, N the number of core electrons, and $P_j(\rho)$ the radial wave functions of the core electrons. For the present calculations, the undistorted core wave functions were taken to be the analytic Hartree-Fock functions[8] of the relaxed ion. In the excited state, the active electron is fairly far removed from the core and sees primarily a Coulomb field. The above method should thus give a good representation for the

TABLE I. Binding energies and scaling parameters for Ar and Kr.

Atom	State	Average binding energy, $\lvert\tilde{E}_{nl}\rvert$ (Ry)	Scaling parameter, a_{nl}
Ar	$3p^5 4s$	0.306 27	1.2718
	$4p$	0.194 64	1.2343
	$3d$	0.127 40	1.2490
	$5s$	0.123 76	1.2512
	$5p$	0.091 83	1.2204
	$4d$	0.071 74	1.2383
Kr	$4p^5 5s$	0.297 00	1.2245
	$5p$	0.185 93	1.1915
	$4d$	0.133 21	1.2228
	$6s$	0.120 06	1.2012
	$6p$	0.088 67	1.1796
	$5d$	0.073 12	1.2104

wave function in the relevant region of configuration space.

The average experimental binding energies were calculated from the formula

$$\tilde{E}_{nl} = \tilde{I} - \left[\sum_J (2J+1)E_{nl,J} \Big/ \sum_J (2J+1)\right] \qquad (14)$$

with $\tilde{I}$ the average ionization energy and $E_{nl,J}$ the excitation energy of each level; all experimental energies for Ar* and Kr* were taken from the NBS tables.[9] The values for E_{nl}, in units of Rydbergs, are given in Table I for the states included in the calculation. The average transition energy ($\langle\langle \Delta E \rangle\rangle$) between two configurations is simply the difference between the values listed in the table. The scaling parameters, obtained from the numerical solution of Eq. (12), are given in the last column of Table I. The fact that all of the values of a_{nl} are close to unity and that the total variation is only $1.18 \lesssim a_{nl} \lesssim 1.27$ provides additional support for the use of the distorted-core approximation for the rare-gas excited states.

III. RESULTS AND DISCUSSION

For metastable argon and krypton, transitions of the type $p^5 n_i s$-$p^5 n_f p$, with $n_f = n_i$, are by far the most important (see below), and both experimental and accurate IC theoretical results for the optical line strengths exist in the literature for these cases.[10-14] Equation (8) has therefore been used to obtain a large number of Born cross sections for the Ar* ($4s$-$4p$) and Kr* ($5s$-$5p$) transition arrays.[15] The effect of choosing different coupling schemes to represent the excited states is shown in Figs. 1 and 2. Referring to the Ar* ($4s$-$4p$) array, Fig. 1 shows the Born cross section versus incident-electron energy for the $1s_2$-$2p_4$ transition

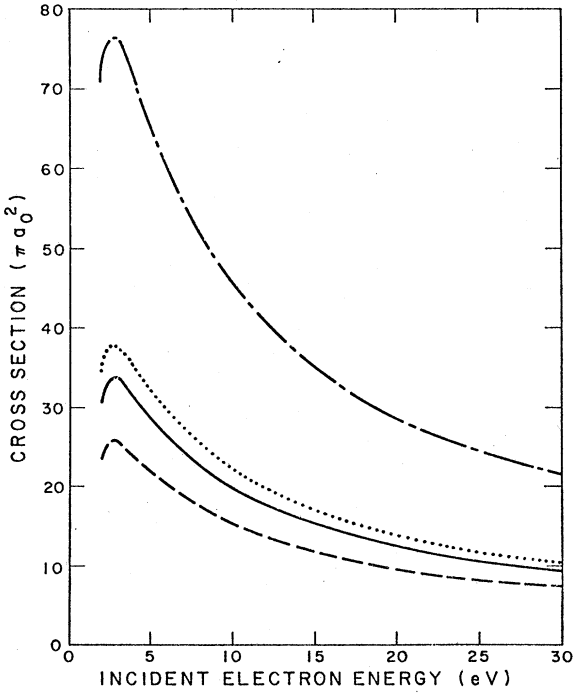

FIG. 1. Born cross section vs incident electron energy for the $1s_2$-$2p_4$ transition of Ar*: Solid line for intermediate coupling, dashed line for jl coupling, long-short-dashed line for LS coupling, dotted line for experimental line strength.

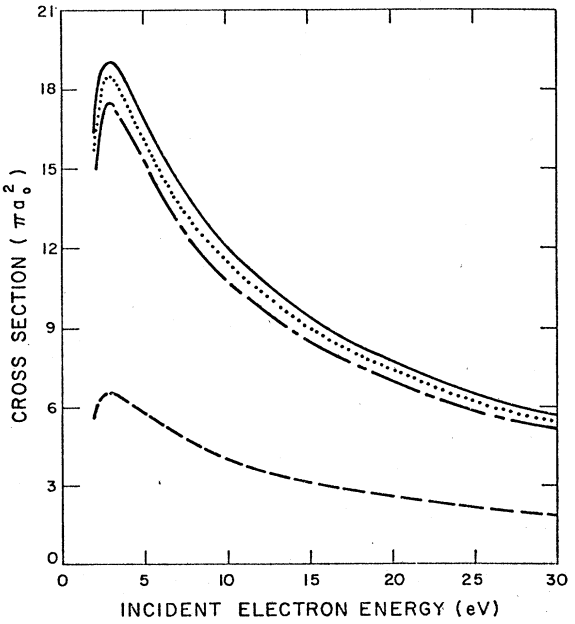

FIG. 2. Born cross section vs incident electron energy for the $1s_5$-$2p_8$ transition of Ar*: Solid line for intermediate coupling, dashed line for jl coupling, long-short-dashed line for LS coupling, dotted line for experimental line strength.

(see Ref. 9 for notation) obtained with the experimental line strength[10] and with the line strengths calculated in intermediate, LS, and jl coupling[11]; Fig. 2 shows the corresponding results for the $1s_5$-$2p_8$ transition. In both cases, the IC results are very close to those obtained using the experimental S values. In the $1s_2$-$2p_4$ case, the pure jl-coupling cross section is in reasonably good agreement with the IC curve, while the LS-coupling cross section is in very poor agreement. For the $1s_5$-$2p_8$ transition, however, just the opposite is true. Furthermore, again with respect to the Ar* ($4s$-$4p$) array, the $1s_2$-$2p_6$ transition is completely forbidden in both jl and LS coupling,[11] while the IC calculation gives a large cross section with a peak value of $36\pi a_0^2$. The cross section clearly can be very sensitive to the choice of coupling scheme, and intermediate coupling should be used to obtain reliable results.

The average Born cross sections, calculated from Eq. (11), are shown as the solid curves in Fig. 3 and 4, for the cases Ar* ($4s$-nl) and Kr* ($5s$-nl). As indicated earlier, the s-p transition with no change in principal quantum number is the dominant process. This is due to the long-range dipole interaction, which causes the s and p states to be strongly coupled and which in turn causes a breakdown in the Born approximation in the low to-intermediate energy range. Seaton has introduced a simplified impact-parameter theory,[16] which accounts approximately for both the weak-coupling and strong-coupling regimes. The method requires a knowledge of the oscillator strength, f and of the cut-off radius,[16] R_0. The average oscillator strength is given by

$$\langle \bar{f}_{n_i s,\, n_f p} \rangle = \tfrac{1}{3} \langle \Delta E \rangle \, |d|^2 , \tag{15}$$

while the cut-off radius was chosen to give agreement with the Born theory at high energies. The parameters used in the calculations were for Ar* ($4s$-$4p$), $\langle f \rangle = 1.068$ and $R_0 = 4.572a_0$; for Kr* ($5s$-$5p$), $\langle f \rangle = 1.121$ and $R_0 = 4.723a_0$. The results of the impact-parameter theory are given by the dashed curve in Figs. 3 and 4. Strong-coupling effects are dominant at incident energies $E_i \lesssim 20$ eV, and the resulting cross sections are seen to differ significantly from the Born theory both in shape and in magnitude.

In some experiments[2,17,18] one measures the so-called optical-excitation cross section, which is

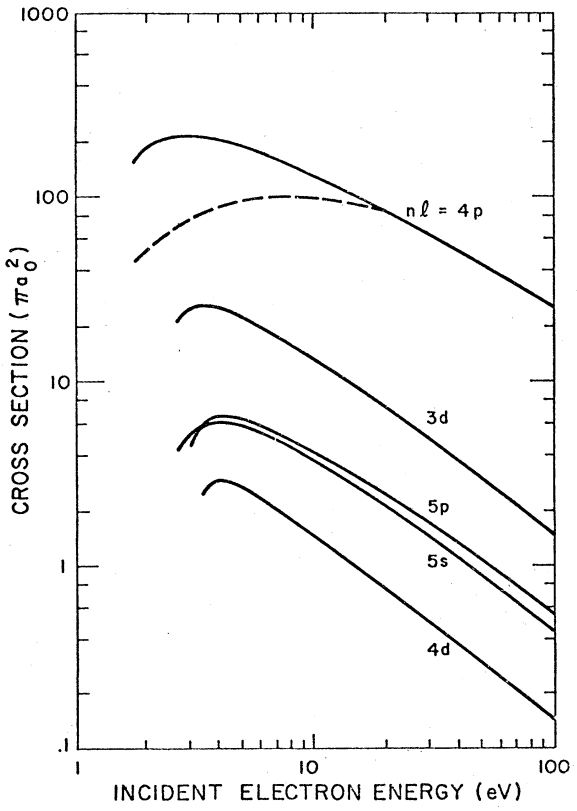

FIG. 3. Average cross section vs incident electron energy for the configurations Ar* ($3p^5 4s$-$3p^5 nl$): solid line for Born theory, dashed line for impact-parameter theory.

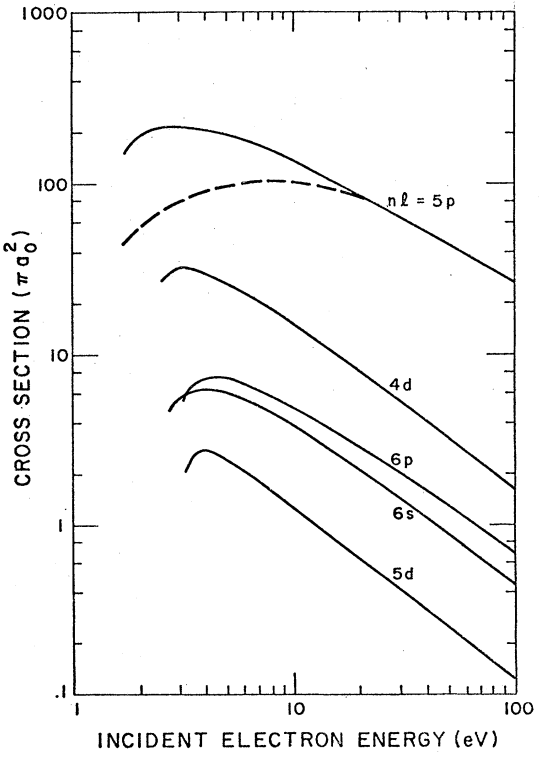

FIG. 4. Average cross section vs incident electron energy for the configurations Kr*($4p^5 5s$-$4p^5 nl$): solid line for Born theory, dashed line for impact-parameter theory.

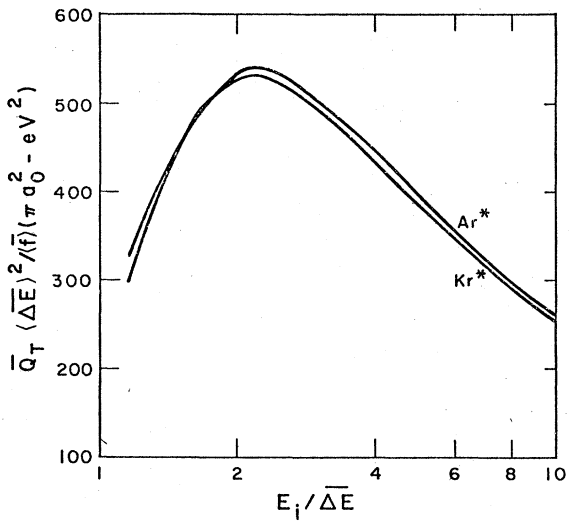

FIG. 5. $\overline{Q}_T \langle \Delta E \rangle^2/\langle f \rangle$ vs $E_i/\langle \Delta E \rangle$ for the transitions Ar* ($4s$-$4p$) and Kr* ($5s$-$5p$). $\overline{Q}_T$ is the average Born cross section including cascades, $\langle \Delta E \rangle$ is the transition energy, $\langle f \rangle$ is the oscillator strength, and E_i is the incident electron energy.

the sum of the direct-excitation cross section plus a contribution due to excitation of and subsequent cascading from higher-lying states. We have therefore considered the average optical excitation cross section, $\overline{Q}_T = \overline{Q}_{\text{direct}} + \overline{Q}_{\text{cascade}}$, for the Ar* ($4s$-$4p$) and Kr* ($5s$-$5p$) transitions. $\overline{Q}_{\text{cascade}}$ can be evaluated from the cross sections given in Fig. 3 and 4; maximum cascade contributions to $\overline{Q}_T$ in the Born approximation are found to be 17% and 18% for argon and krypton, respectively. Following Chen and Gallagher,[17,18] we have plotted the reduced quantities $\overline{Q}_T \langle \Delta E \rangle^2/\langle f \rangle$ vs $E_i/\langle \Delta E \rangle$ in Fig. 5. These curves are very similar to the analogous Born curves for the resonance transitions in the alkalis,[18] which is not surprising given the similarity between the electronic structure of the alkalis and that of the rare-gas metastables. It should be pointed out that we have neglected the complicated branching ratios for the excited states in determining the cascade contribution [for example, the $J=1$ components of the p^5s and p^5d series can decay to the rare-gas ground state as well as to the $np^5(n+1)p$ state]. This leads us to overestimate $\overline{Q}_{\text{cascade}}$, but is compensated for by the fact that we have neglected the additional small contribution due to still higher-lying states not included in the present calculations. Considering these two effects, we estimate that the curves of Fig. 5 are uncertain by ~3%. Based upon measurements of a number of optically allowed electron-impact excitation cross sections, Chen and Gallagher[17,18] have suggested an empirical universal relation of the form

$$Q_T^{(\text{obs.})}/Q_T^{(\text{Born})} \approx 1 - (\Delta E/E_i)^{1/2} \tag{16}$$

which would imply that the Born theory is no worse than a factor of 2 in error for incident energies as low as $E_i \sim 6$ eV for the present case. Moreover, Seaton's method[16] appears capable of removing ~ $\frac{3}{4}$ of the discrepancy between the observed and Born cross sections in this energy range.

IV. CONCLUSION

Electron-impact excitation processes for metastable argon and krypton atoms have been considered. General formulas for the Born cross section in intermediate coupling have been given, from which various special cases were obtained (i.e., for s-p transitions and for the average cross section between two configurations). The importance of using intermediate coupling, as compared to various pure-coupling schemes, has been pointed out. Strong-coupling effects were shown to be dominant at low-to-intermediate energies for the Ar* ($4s$-$4p$) and Kr* ($5s$-$5p$) dipole transitions, which were found to have large cross sections with peak values ~ $100\pi a_0^2$. Finally, the range of application of the Born approximation was estimated from an empirical point of view through a consideration of the optical excitation function.

ACKNOWLEDGMENTS

The author wishes to acknowledge helpful discussions with M. J. W. Boness and A. C. Gallagher. This work was supported by the Advanced Research Projects Agency of the Department of Defense and monitored by ONR under Contract No. N00014-75-C-0064.

[1] J. H. Jacob and J. A. Mangano, Appl. Phys. Lett. 28, 724 (1976).

[2] Preliminary results of an experiment to measure cross sections for electron-impact excitation of metastable krypton were discussed by M. J. W. Boness at the 30th Annual Gaseous Electronics Conference, Palo Alto, California (October 1977) (unpublished). A complete description of the experiment and resulting krypton cross sections will be published in the near future.

[3] B. L. Moiseiwitsch and S. J. Smith, Rev. Mod. Phys. 40, 238 (1968).

[4] E. U. Condon and G. H. Shortley, *The Theory of Atomic Spectra*, (Cambridge U. P., Cambridge, England, 1964).

[5] R. D. Cowan and K. L. Andrew, J. Opt. Soc. Am. 55,

502 (1965).
[6]A. R. Edmonds, *Angular Momentum in Quantum Mechanics,* (Princeton U. P., Princeton, N. J. 1960).
[7]L. A. Vainshtein, Opt. Spectrosc. 3, 313 (1957).
[8]E. Clementi and C. Roetti, At. Data Nucl. Data Tables 14, 177 (1974).
[9]C. E. Moore, *Atomic Energy Levels,* U. S. Nat. Bur. Stand. Circ. No . 467 (U. S. Dept. of Commerce, Washington, D. C., 1949), Vols. I and II.
[10]W. L. Wiese, M. W. Smith, and B. M. Miles, *Atomic Transition Probabilities,* NSRDS-NBS 22 (U. S. Dept. of Commerce, Washington, D. C. 1969); Vol. II.
[11]R. H. Garstang and J. VanBlerkom, J. Opt. Soc. Am. 55, 1054 (1965).
[12]P. W. Murphy, J. Opt. Soc. Am. 58, 1200 (1968).
[13]R. A. Lilly, J. Opt. Soc. Am. 66, 245 (1976)
[14]The authors of Refs. 11–13 give transition probabilities or Einstein A factors in intermediate coupling. The corresponding line strength, in atomic units, is obtained from the relation $S = 4.95 \times 10^{-19}\, g_u \lambda^3 A$, with g_u the statistical weight of the upper level, λ the transition wavelength in Å, and A the transition probability in $\sec^{-1}$
[15]H. A. Hyman (unpublished).
[16]M. J. Seaton, Proc. Phys. Soc. 79, 1105 (1962).
[17]S. T. Chen and A. C. Gallagher, Phys. Rev. A 14, 593 (1976).
[18]S. T. Chen and A. C. Gallagher, Phys. Rev. A 17, 551 (1978).